Modeling the exoplanet population of the solar vicinity with a cosmological galaxy simulation

Author: Artur Viñas Ferran.
Facultat de Física, Universitat de Barcelona, Diagonal 645, 08028 Barcelona, Spain.

Advisor: Friedrich Anders, Chloé Padois, Daniel del Ser
(Dated: January 14, 2024)

Abstract: This work aims to simulate a realistic habitable exoplanetary population through state-of-the-art models. It analyses various factors that influence the habitability of exoplanets, such as the host stellar mass, stellar metallicity, stellar birth position, stellar age, and the semi-major axis of the planet's orbit. The results obtained are then compared with the known exoplanetary population sourced from the NASA Exoplanetary Archive (NASA 2023). Remarkable results have been obtained in the host star's metallicities, as a common negative metallicity tendency is observed in NASA's habitable planets, as well as in the simulation developed in this work. A percentage of habitable exoplanets within the initially presented population of approximately $\sim 2\%$ has been determined, while the current percentage of habitable exoplanets among the discovered population to date is approximately $\sim 1.5\%$.

I. INTRODUCTION

The discovery, exploration, and study of exoplanets have started a new era in astrophysics. This new field of exploration has reached remarkable advancements in recent years through innovative observation techniques, such as better precision in radial velocity measurements, transmission spectroscopy, or direct imaging. After 30 years of exoplanetary exploration, more than 5000 exoplanets have been discovered through diverse observational techniques.

Several missions have been sent to explore the current exoplanetary population in our surroundings. The most successful have been the Kepler Space Telescope (Borucki et al. 2010), the Planetary Transits and Oscillations of stars (PLATO; Rauer et al. 2014), the James Webb Space Telescope (JWST; McElwain et al. 2023), the Transiting Exoplanet Survey Satellite (TESS; Pál et al. 2018), and the High-Accuracy Radial Velocity Planetary Searcher (HARPS; Mayor et al. 2003). The first four missions focus on studying Earth-like planets through planetary transits while the last works with radial velocities. It has to be mentioned that the current discovered exoplanetary population was mainly detected by Kepler's mission (over 2600; Borucki et al. 2010), which studied a very concrete portion of the Milky Way (MW) from the constellations of Cygnus and Lyra. Kepler was also the best-equipped mission, boasting the most precise observations to date. Consequently, the current exoplanetary archive is affected by observational biases that must be taken into account.

Most of the exoplanetary systems discovered to date do not resemble our solar system. This can be explained by the limitations of the current observational techniques, which are restricted to short periods and more massive planets. Current surveys indicate that small planets are more common than giant planets. The occurrence rate of giant planets tends to increase with longer orbital periods, as well as increase with the hosting star's metallicity and mass (Madau 2023). It has also been observed that multiplanetary systems with regular spacing and size similarity are very common. One of the current state-of-the-art main themes is called the *Radius Gap* (Fulton et al. 2017; Owen & Wu 2017), which consists of an observed depopulation of exoplanets between 1.5 and 2 times Earth's radius. This is likely caused by photoevaporation driven mass loss, where energetic radiation ionizes the gas and causes it to disperse away from the ionizing source. This gap has also a variability with the spectral type (McDonald et al. 2019; Zeng et al. 2017).

The search for habitable worlds and extraterrestrial life has been a point of interest for modern science, presenting one of the primary mysteries of our century. The ongoing search for signs of life is primarily based on the assumption that extraterrestrial life shares fundamental characteristics with life on Earth, with carbon-based chemistry, and a dependence on liquid water as a solvent Kaltenegger (2017). The main factors that are believed to determine those conditions include the properties of the hosting star, such as its spectral type, metallicity, and age. The planet's orbital radius must also be taken into consideration, as it influences the amount of radiation the planet will receive. Additionally, the potential risk of supernovae (SN) should be considered, as these violent processes lead to impossible conditions for any kind of life, based on our current understanding. Consequently, when assessing habitability, the position of the stellar system in the galaxy where the exoplanet is located must be taken into account.

This work aims to simulate a simple but realistic habitable exoplanet population by applying the main known factors that influence the existence of Earth-like planets.

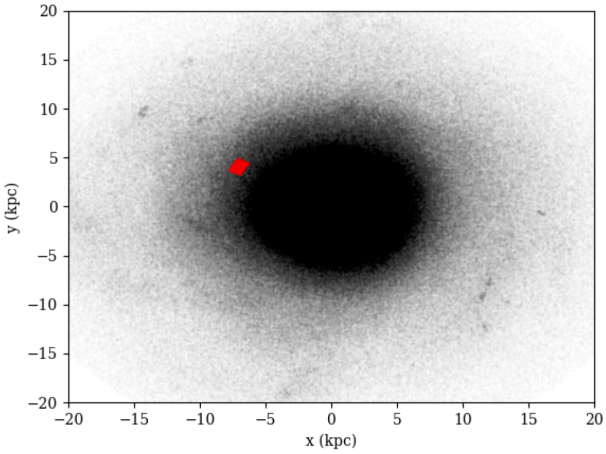

FIG. 1: Representation on the xy plane (the galactical plane) of the g7.55e11 particle bins positions (in black) and the solar neighborhood selected in our simulation (in red).

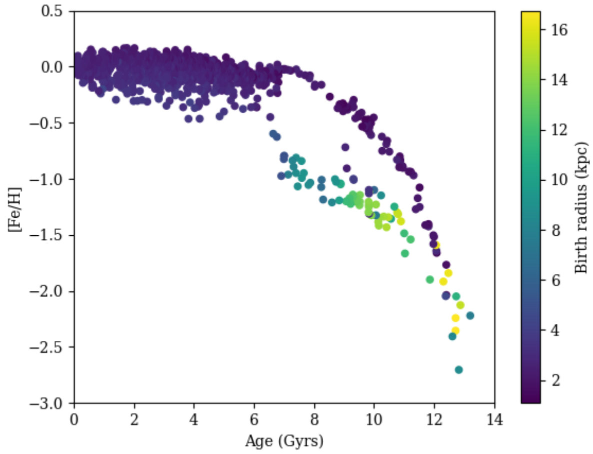

FIG. 2: Diagram of the metallicities of the star particles on the selected solar neighborhood vs their age and birth radius.

II. METHODOLOGY

A. Cosmological simulation and solar neighborhood

Our starting point was the NIHAO-UHD suite of cosmological hydrodynamical simulations of Milky Way (MW) mass galaxies (Buck et al. 2020). This suite takes into account six distinct cosmological simulations: each one for dark matter particles, gas particles, and stellar particles. In this context, we were interested in the last ones, as they are used as virtual particles employed to trace the stellar density field to represent simple stellar populations of thousands of stars. We selected the simulated galaxy g7.55e11 of stellar particles as the initial density distribution of our simulation of exoplanetary hosting stars. This simulation provides enough stellar particles (over $4 \cdot 10^6$) that reproduce stellar disc properties such as stellar mass, size, and rotation curve, which agree well with observations of the MW and local galaxies.

A similar environment to the solar system was implemented by selecting the solar neighborhood, which was defined (in cylindrical coordinates) with an inclination of $(30 \pm 5)^\circ$ to the galactic bar, a galactocentric radius of 7.7 to 8.7 kpc, and a maximum distance to the disk plane of 0.5 kpc (loosely based on Bland-Hawthorn & Gerhard 2016).

B. From star particles to stars

The stars simulated in this work were generated following Chabrier's Initial Mass Function (IMF) Chabrier (2003) using the solar neighborhood star particles. Initially, late F to early M stars were considered due to conditions similar to those in our planetary sample. OBA stars were excluded for several reasons: Firstly, their lifetimes are too short compared to the time required for life processes (several Gyr on Earth). Secondly, Reffert et al. (2013) concludes that higher mass stars do not form giant planets which are observable at separations of a few *au* today. Possible reasons include slower growth, longer migration time scale, and faster disk depletion. Thirdly, planets orbiting them are harder to detect. This can be explained by the difficulty of detecting exoplanets around massive stars using current techniques. Exoplanetary exploration through transit photometry or radial velocities in massive stars becomes challenging with the resolutions currently available (Assef et al. 2009); therefore, more precise instrumentation and techniques are required. Ultimately, late-M stars were ruled out due to the violence of their initial phases, leading to the complete evaporation of water on their planets, resulting in highly improbable conditions for life(Kaltenegger (2017)).

In this simulation, stars were generated with masses ranging from 0.08 to $1.6 M_\odot$ solar masses. Both Kroupa's (Kroupa 2002) and Chabrier's (Chabrier 2003) Initial Mass Functions (IMFs) were considered to describe our star population. Finally, Chabrier's IMF was selected as it better captures the range of masses proposed.

C. Binary stars

Binary stars were not considered in this work, as they are systems with complex processes that show a wide variety of instabilities, often impacting the stability of the planetary system. The sample selection of non-binary stars was done based on their simulated masses, using

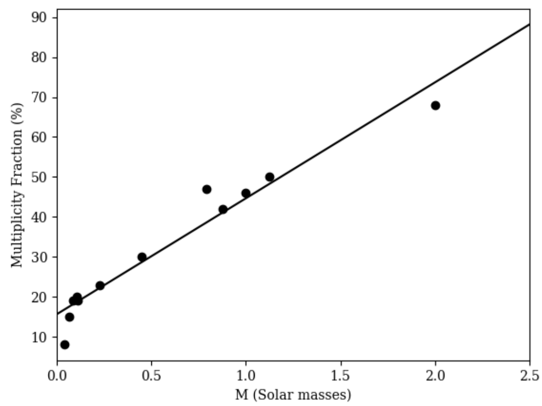

FIG. 3: Multiplicity fraction for stars from 0 to $2.5M\odot$ from Offner et al. (2023) surveys. Its linear trend is also represented (Equation 1).

the latest surveys on binary systems of main-sequence stars (Offner et al. 2023). The multiplicity fraction (MF) is defined as the number of binary or higher-order systems observed for stars of a determined mass.

Using the data provided in those studies Offner et al. (2023) (showed in 3) we obtained the following linear relation:

$$M(m) = 29.02 \cdot m + 15.62 \tag{1}$$

This relation has a correlation factor of $R^2 = 0.95$.

This probability distribution was applied to our star population. In consequence, all those stars that had high probability of being binaries were removed from our sample.

D. Simulating exoplanets

The occurrence rate is the average number of planets per star for a concrete star population. Bryson et al. (2020) derives that the occurrence rate of Earth-like planets with radii between 0.5 and $1.5R_\oplus$ orbiting stars with effective temperatures between 4800 and 6300K is:

$$0.37^{+0.48}_{-0.21} < \eta_\oplus < 0.60^{+0.90}_{-0.36} \tag{2}$$

For simplicity, in this work, it was assumed one planet per simulated star. The semi-major axis of each planet was drawn from a random uniform distribution bounded by the radius of its star and the equivalent Jupiter orbit radius (relative to the stellar radius). The radius of each planet was obtained using a random uniform distribution bounded by the equivalent radius of Mercury and Jupiter (relative to the stellar radius).

Planets with radii not ranging from 0.5 to $2R_\oplus$ were excluded from the study, as this range of radii represents

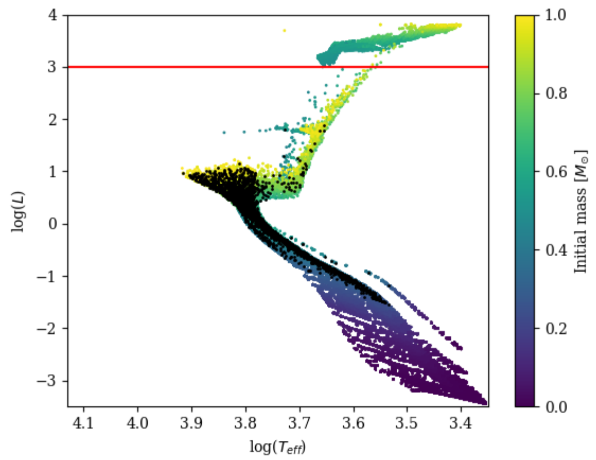

FIG. 4: HR diagram of the initial star population generated (in color) and the hosting stars of the simulated habitable planets (in black). The $log(L) = 3$ limit is also plotted. Both distributions were obtained through the isochrones matching.

the most probable exoplanet population capable of supporting life within their habitable zones (Super-Earths).

E. Determination of the Habitable Zone (HZ) through isochrone matching

The Hertzsprung–Russell (HR) diagram is a very common representation used in astrophysics that shows the relationship between the stars' absolute luminosities (or absolute magnitudes) versus their effective temperatures (or stellar classifications).

An isochrone is the curve that a group of stars of a certain age and chemical composition describes in an HR diagram. These mass sequences are obtained from stellar evolution models and provide information about the star's astrophysical parameters (effective temperature, surface gravity, luminosity, etc.). In this step, all the stars resulting from the previous processes were matched to their corresponding PARSEC isochrones (Marigo et al. 2017). The process involved finding the point on the isochrones that best fit the known properties of each star (in our case, the mass, age, and metallicity of the star). From there, their luminosities and effective temperatures were determined.

As can be seen in 4, a group of massive stars appears in the HR diagram above the value of $log(L) = 3$, which does not match with any kind of stars that are expected on an HR diagram. This can be explained by the fact that these massive stars are probably dead. Due to this observation, stars with $log(L) \geq 3$ were removed from the simulation.

The Habitable Zone (HZ) of a star is the range of distances from a star where a planet can be considered a candidate to harbor life. The computation of this zone is primarily based on the possibility of a planet having temperatures that allow the existence of liquid water Kaltenegger (2017). The Habitable Zone can also be considered in terms of insolation (S_{in} and S_{out}). If a planet experiences insolations outside the minimum or maximum values of its star's HZ, it is not expected to harbor life.

Through isochrone matching, from which effective temperatures and luminosities were obtained, it was possible to compute the internal and external boundaries of the Habitable Zone (HZ) for each star according to the following equation extracted from Kaltenegger (2017):

$$S_{eff} = S_{Sun} + aT + bT^2 + cT^3 \tag{3}$$

Where S_{eff} and S_{Sun} are the Effective Flux Boundary of the star and the Sun, T is related to the effective temperature of the star $T = T_{eff} - 5780$ K, and a, b and c are parameters obtained in the mentioned work.

TABLE I: Values used to compute the internal and external Effective Flux Boundary of each star in equation 3.

	S_{Sun}	a	b	c
IN	1.7665	1.3351×10^{-4}	3.1515×10^{-9}	$-3.3488 \times 10-12$
OUT	0.324	5.3221×10^{-5}	1.4288×10^{-9}	-1.1049×10^{-12}

After computing the HZ of all stars simulated, the insolation that each planet faces (I) was determined according to the following equations (also extracted from Kaltenegger (2017)), where L is the star's luminosity:

$$L = R_s^2 \times \left(\frac{T_{eff}}{5778}\right)^4 \tag{4}$$

$$I = \left(\frac{L}{a}\right)^2 \tag{5}$$

Where R_s is the stellar radius, a the semi-major axis of the planet's orbit, and T_{eff} the effective temperature of the star.

From there, all the planets simulated whose insolation was out of its host star HZ [S_{in}, S_{out}] were deleted from the sample.

III. RESULTS

This work began with an initial population of 4556857 star particles, derived from the simulated galaxy g7.55e11 (Buck et al. 2020). After defining the solar neighborhood, 1147 star particles were selected, and 681450 stars were subsequently generated according to Chabrier's IMF (Chabrier 2003). Binary stars (508958), old stars (6005), and young stars (any star under 10 Myears was found) were excluded from the simulation, leaving 166487 stars. Among these stars, 166487 exoplanets were generated, with one assigned to each star. Finally, any exoplanets not located within their respective Habitable Zones (HZ) and with radii out of 0.5 to $2R_{\oplus}$ were removed from the simulation. The final result yielded a population of 3707 exoplanets, representing potential candidates for hosting life. The current percentage of habitable exoplanets among all the discovered exoplanets to date is approximately $\sim 1.5\%$. In this simulation, the percentage of habitable planets within the initially presented population is approximately $\sim 2\%$, which is a good approach to reality.

The exoplanetary population obtained in this work is expected to show realistic properties in terms of metallicity, effective temperatures, radius of the planets and semi-major axis of their orbits.

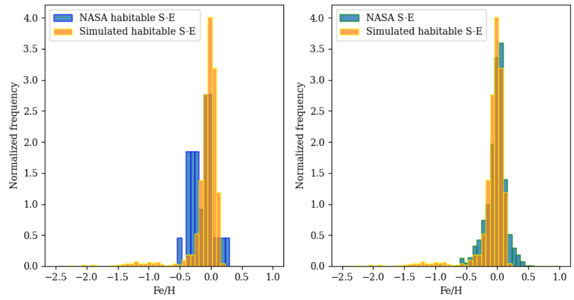

FIG. 5: On the left side, the metallicity histogram of the simulated exoplanetary hosting stars vs the one related to NASA's habitable Super-Earths NASA (2023). On the right side, the metallicity histogram of the simulated exoplanetary hosting stars vs the one related to NASA's Super-Earths.

A. Metallicities

The host star's metallicity is one of the main factors that determine the possibility of stellar systems having Earth-like planets (Madau 2023). In this section, we study the histogram of metallicities obtained from our habitable planets vs the ones observed in NASA (2023) with a general sample, and another with only the habitable planets.

It was expected to obtain analog distributions of metallicities in the histograms about habitable exoplanets from NASA (2023) and our simulation 5. The histogram of our simulation shows a sharper pick than both of NASA's histograms over the 0.0 [Fe/H] maximum. On the other side, an increase of exoplanets with negative metallicities is observed in NASA's habitable exoplanets histogram, mirroring the trend observed in our simulation's histogram. This population of negative metallicities can be a real tendency in nature or a consequence of our calculations and assumptions on the HZ.

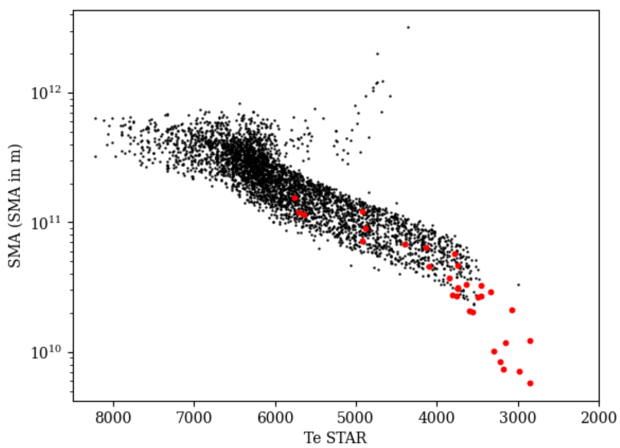

FIG. 6: Effective temperature of the host stars population vs its exoplanets' semi-major axis orbit for the simulated habitable exoplanet population (in black), and NASA's Exoplanetary Arxiv habitable exoplanets NASA (2023) (in red). The y-axis is presented in a logarithmic scale, and the x-axis is inverted.

B. Effective temperatures

Effective temperatures of the hosting stars are compared with the semi-major axis of the planet's orbits on a logarithmic scale. A similar distribution to an HR diagram is observed: One main branch shows an exponential relation between effective temperatures and the orbits' semi-major axis of the planets. A secondary and more diluted branch is observed with an inverted direction to the main one, which corresponds to the planet's population that is hosted by giant stars. Both simulated and NASA's distributions show similar characteristics in this diagram. However, NASA's habitable planets have smaller orbits compared to the majority of the simulated exoplanets in this study.

IV. CONCLUSIONS & FUTURE WORK

This work can be understood as a first step in exoplanetary simulation. It was aimed to obtain a realistic habitable population of Super-Earths, expected to show characteristics similar to those discovered to date. Remarkable results have been obtained in the host stars' metallicities. A tendency of habitable planets to be hosted by stars metallically negative is observed in our simulation along with NASA's discovered habitable planets. Future studies will corroborate this phenomenon as a natural tendency in nature, or just a mere consequence of our calculations and assumptions on the HZ.

A percentage of habitable exoplanets within the initially presented population of approximately $\sim 2\%$ has been determined, while the current percentage of habitable exoplanets among the discovered population to date is approximately $\sim 1.5\%$.

A potential line for future research in this work could involve formulating a more precise occurrence rate when generating the exoplanet population. Other ways of determining the planet's radius and semi-major axis could be explored. Furthermore, when establishing habitability conditions, other factors, such as the chemical composition of exoplanets' atmospheres, and the risk factor associated with supernovae (SN) in stellar systems, due to their location in the galactic disc, could be considered.

Kirkpatrick et al. (2023) recently revealed that Chabrier's IMF overestimates the number of stars for masses lower than $0.2M_\odot$. More realistic results would be obtained by defining the IMF in this range of masses more precisely.

Assef, R. J., Gaudi, B. S., & Stanek, K. Z. 2009, ApJ, 701, 1616
Bland-Hawthorn, J. & Gerhard, O. 2016, ARA&A, 54, 529
Borucki, W. J., Koch, D., Basri, G., et al. 2010, Science, 327, 977
Bryson, S., Coughlin, J., Batalha, N. M., et al. 2020, AJ, 159, 279
Buck, T., Obreja, A., Macciò, A. V., et al. 2020, MNRAS, 491, 3461
Chabrier, G. 2003, PASP, 115, 763
Fulton, B. J., Petigura, E. A., Howard, A. W., et al. 2017, AJ, 154, 109
Kaltenegger, L. 2017, ARA&A, 55, 433
Kirkpatrick, J. D., Marocco, F., Gelino, C. R., et al. 2023, arXiv e-prints, arXiv:2312.03639
Kroupa, P. 2002, Science, 295, 82
Madau, P. 2023, ApJ, 957, 66
Marigo, P., Girardi, L., Bressan, A., et al. 2017, ApJ, 835, 77
Mayor, M., Pepe, F., Queloz, D., et al. 2003, The Messenger, 114, 20
McDonald, G. D., Kreidberg, L., & Lopez, E. 2019, ApJ, 876, 22
McElwain, M. W., Feinberg, L. D., Perrin, M. D., et al. 2023, PASP, 135, 058001
NASA. 2023, NASA Exoplanetary Arxiv
Offner, S. S. R., Moe, M., Kratter, K. M., et al. 2023, 534, 275
Owen, J. E. & Wu, Y. 2017, ApJ, 847, 29
Pál, A., Molnár, L., & Kiss, C. 2018, PASP, 130, 114503
Rauer, H., Catala, C., Aerts, C., et al. 2014, Experimental Astronomy, 38, 249
Reffert, S., Bergmann, C., Quirrenbach, A., Trifonov, T., & Künstler, A. 2013, in Protostars and Planets VI Posters
Zeng, L., Jacobsen, S. B., & Sasselov, D. D. 2017, Research Notes of the American Astronomical Society, 1, 32